T-type channels control the opioidergic descending analgesia at the low threshold-spiking GABAergic neurons in the periaqueductal gray

Cheongdahm Park[a,b], Jong-Hyun Kim[a,b], Bo-Eun Yoon[a,c], Eui-Ju Choi[b], C. Justin Lee[a,c], and Hee-Sup Shin[a,1]

[a]Center for Neural Science, Future Fusion Technology Laboratory, Korea Institute of Science and Technology, Seoul 136-791, Korea; [b]National Creative Research Initiative Center for Cell Death, Graduate School of Biotechnology, Korea University, Seoul 136-701, Korea; and [c]Neuroscience Program, University of Science and Technology, Daejeon 305-701, Korea

Endogenous opioids generate analgesic signals in the periaqueductal gray (PAG). However, because cell types in the PAG are difficult to identify, its neuronal mechanism has remained poorly understood. To address this issue, we characterized PAG neurons by their electrical properties using differentially labeled GABAergic and output neurons in the PAG. We found that GABAergic neurons were mostly fast-spiking cells and could be further divided into two distinct classes: with or without low-threshold spikes (LTS) driven by T-type channels. In contrast, the PAG output neurons lacked LTS and showed heterogeneous firing patterns. To reveal the function of the LTS, we examined the mutant mice lacking the α1G T-type channels (α1G$^{-/-}$). The mutant mice lacked LTS in the fast-spiking GABAergic neurons of the PAG and unexpectedly showed impaired opioid-dependent analgesia; a similar phenotype was reproduced in PAG-specific α1G-knockdown mice. Electrophysiological analyses revealed functional expression of μ-opioid receptors in the low threshold-spiking GABAergic neurons. These neurons in the mutant lacking LTS showed markedly enhanced discharge activities, which led to an augmented inhibition of output neurons. Furthermore, the impaired analgesia observed in α1G$^{-/-}$ mice was reversed by blocking local GABA$_A$ receptors. These results indicate that α1G T-type channels are critical for the opioidergic descending analgesia system in the PAG.

opioid-descending analgesia | α1G | morphine | stress | calcium-activated potassium channel | afterhyperpolarization

Endogenous opioids generate analgesic signals in the periaqueductal gray (PAG) (1–6). These signals are projected to and relayed by the rostral ventromedial medulla (RVM) to the dorsal horn of the spinal cord (SC), which is called descending analgesia circuit. Swimming in warm water induces opioid-dependent swim stress-induced analgesia (SSIA) along this circuit (7). Morphine, an agonist of primarily μ-opioid receptors (μORs), hyperpolarizes neurons by increasing potassium conductance and inhibiting voltage-gated calcium conductance, which collectively inhibit spike firing and decrease neurotransmitter release (8, 9). Because this inhibitory effect of morphine paradoxically excites PAG output neurons projecting to the RVM, a disinhibition model has been proposed in which opioids produce antinociceptive signals in the PAG by directly inhibiting tonically active GABAergic neurons, thereby disinhibiting the PAG-RVM projection neurons (1, 2, 5, 10). Cell type-specific electrophysiological evidence to support this hypothesis is sparse, however, because it is difficult to distinguish their cell types based on morphology or electrophysiological properties.

Pain signals are modulated by the descending analgesic circuit as well as the ascending sensory circuit. Evidence indicates that opioid antinociception is associated with alterations in calcium influx through voltage-gated Ca^{2+} channels, including low voltage-activated T-type channels (11, 12). Our previous studies revealed a role of T-type channels in the pain ascending sensory pathway by showing that this channel inhibits pain signals at the supraspinal level (13, 14).

However, whether T-type channels would play a role in the opioidergic descending analgesia pathway is an open question.

In this study, we provide evidence that α1G T-type channels control the opioidergic descending analgesia system at the unique population of low threshold-spiking, μOR-positive GABAergic neurons in the PAG.

Results

GABAergic Neurons Are Localized in the Caudal Portion of the Ventrolateral Column, Whereas PAG-RVM Projection Neurons Consist of Distinct Longitudinal Columns in the Mouse PAG. GABAergic neurons and PAG-RVM projection neurons generate analgesic signals. To identify those neurons, we injected a retrograde tracer into the RVM in glutamate decarboxylase 67 (GAD67)-GFP transgenic mice for the labeling of GABAergic neurons and PAG-RVM projection neurons in the PAG (Fig. S1). Serial sections of the PAG revealed that GFP-positive GABAergic neurons were localized only in the caudal portion of the ventrolateral PAG (Fig. 1 B and D and Table S1). PAG-RVM projection neurons are distributed to three anatomically distinct longitudinal columns in the mouse PAG: one in the dorsomedial (DM) region and two each in bilaterally located lateral/ventrolateral (L/VL) regions. In contrast, dorsolateral (DL) PAG region lacks projection neurons (Fig. 1 C and E). This is similar to that reported for rat brains (6). However, none of the GFP-positive GABAergic neurons were colocalized with the retrograde labels in confocal z-scan analyses (Fig. 1 F–I and Fig. S2). From these results, we identified two mutually exclusive cell types in the mouse PAG: local GABAergic neurons and non-GABAergic projection neurons.

Low-Threshold Spikes Are Selectively Induced in a Subgroup of GABAergic Neurons but Are Absent in Projection Neurons. The identified cell types in the PAG allowed us to characterize their electrical properties. We focused on the caudal portion of the VL region owing to its known sensitivity to morphine in vivo and the confined localization of GABAergic neurons in this region (Fig. 1). Based on responses to depolarizing or hyperpolarizing current pulses, we classified PAG neurons into distinct types: fast-spiking (FS) and transient-spiking (TS) with or without low-threshold spikes (LTS).

We found that most GABAergic neurons (31 of 33 cells) formed a relatively homogeneous population of the FS type (Fig. 2A). The remaining GABAergic neurons (2 of 33 cells) were of the TS type. Using hyperpolarizing pulses, we found that FS GABAergic neurons were approximately evenly split between those that exhibited LTS (16 of 31 cells) and those that did not (15 of 31 cells). PAG-RVM
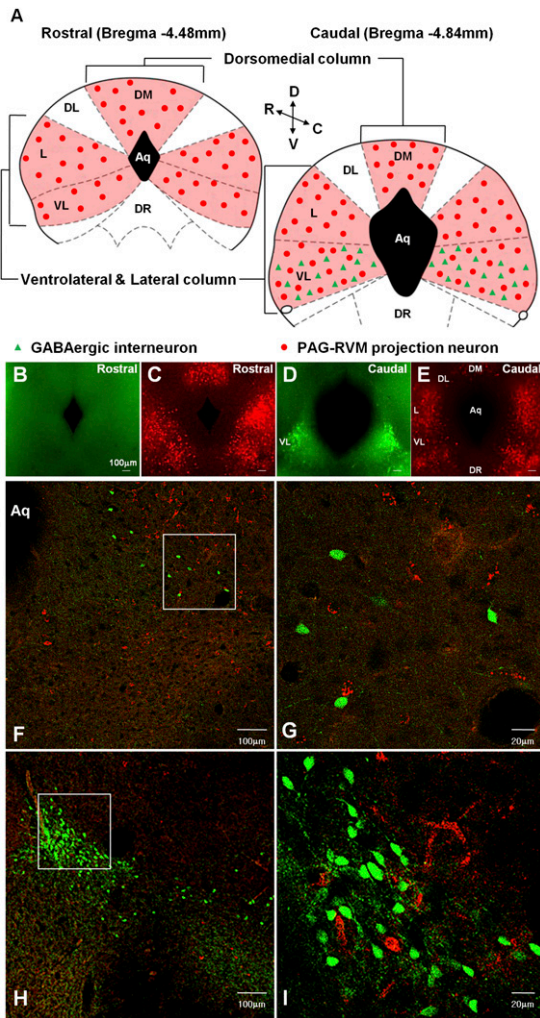
NEUROSCIENCE

Fig. 1. The localized GABAergic neurons in the caudal part of the VL column and the distinct longitudinal columns of PAG-RVM projection neurons in the mouse PAG. (*A*) The cartoons illustrate the distribution of the GABAergic neurons and PAG-RVM projection neurons in the mouse PAG. The colored areas indicate the position of PAG-RVM projecting columns. (*B–E*) The sections of the PAG are presented with epifluorescence using a GFP (*B* and *D*) and a rhodamin (*C* and *E*) filter. (*F–I*) Confocal imaging. (*F* and *H*) The GABAergic neurons in the VL column are localized only in the caudal portion (*F*) and become denser up to the end of the caudal portion (*H*). (*G* and *I*) The enlarged view in *Inset* in *F* and *H* is shown in *G* and *I*, respectively. Green, the GFP on GABAergic neurons; red, the retrograde dye on PAG-RVM projection neurons.

projection neurons were then categorized into two groups; 7 of 12 cells were FS type (Fig. 2*C*), and 5 of 12 cells were TS type (Fig. 2*E*). In contrast to the GABAergic neurons, however, LTS neurons were not apparent in either of these projection neuron subpopulations.

The selective presence of LTS in a subgroup of GABAergic neurons prompted us to study the function of LTS in the PAG. Of the three subtypes of T-type channels that are known to induce LTS, the α1G subunit was the most likely candidate for LTS in PAG neurons, because the α1G subunit, not α1H or α1I, is predominantly expressed in the PAG, but not in the RVM of the rat (15), and is confirmed in the mouse (Fig. S3). The crossing of GAD67-GFP mice with mice lacking the T-type channel α1G (Ca$_V$3.1) subunit (16) revealed that α1G subunit is the sole mediator of LTS in the GABAergic neurons of the wild-type PAG. Similar to wild-type mice, most GFP-positive GABAergic neurons (26 of 28 cells) were the FS type (Fig. 2*B*), and only a small mi-

nority (2 of 28 cells) were TS type. There was no GABAergic neuron exhibiting LTS in the α1G$^{−/−}$ PAG. The firing patterns of PAG-RVM projection neurons in α1G$^{−/−}$ mice (FS type, nine cells; shown in Fig. 2*D*; TS type, five cells; shown in Fig. 2*F*) were similar with those of the wild type. Other neuronal properties were not significantly different between the two genotypes (Table S2). This confirms that the α1G T-type channel is selectively expressed in low threshold-spiking GABAergic neurons.

Opioid-Dependent Analgesia Is Impaired in α1G$^{−/−}$ Mice as Well as in PAG-Specific α1G-Knockdown Mice. The electrophysiological characteristics of GABAergic neurons in the PAG prompted us to examine the function of LTS of these neurons in opioidergic analgesia. First, we examined the baseline thermal sensitivity of α1G$^{−/−}$ as well as PAG-specific α1G knockdown mice. The knockout or PAG-specific knockdown of α1G did not significantly affect baseline thermal sensitivity (Fig. 3*A*). Next, we tested the performance of those mice in an opioid-dependent SSIA assay. Unexpectedly, we found that the SSIA was significantly impaired in α1G$^{−/−}$ mice compared with wild-type mice, which was reproduced in PAG-specific α1G-knockdown mice (Fig. 3*B*). In postmortem examinations of brains after SSIA assays, we observed a 33.33% ± 1.31% reduction in α1G-targeted neuronal cells of the PAG in shRNA-α1G mice compared with control mice (10 slices/group; $P < 0.0001$) (Fig. S4). These results indicate that α1G T-type channels in the PAG are required for the expression of SSIA but not for basal thermal-pain sensation.

Next, morphine-induced analgesia was evaluated by systemic injection (10 mg/kg) and PAG-specific infusion (1 µg) through a cannula (Fig. S5). In wild-type mice, morphine induced robust analgesia compared with saline-treatment controls [systemic: $F_{1,13} = 33.406$, $P < 0.001$, repeated-measures (RM) ANOVA, shown in Fig. 3*C*; PAG: $F_{1,19} = 43.455$, $P < 0.001$, RM ANOVA, shown in Fig. 3*E*]. In the α1G$^{−/−}$ mice, morphine also induced a significant analgesic effect compared with saline controls (systemic: $F_{1,13} = 11.428$, $P < 0.01$, RM ANOVA, shown in Fig. 3*D*; PAG: $F_{1,17} = 6.628$, $P < 0.05$, RM ANOVA, shown in Fig. 3*F*). However, the extent of this analgesia was substantially less than that in wild-type mice (systemic: $F_{1,11} = 10.752$, $P < 0.01$, RM ANOVA; PAG: $F_{1,14} = 11.179$, $P < 0.01$, RM ANOVA). The comparison at the peak also showed significant impairment of analgesia in mutant mice after PAG injections (Fig. 3*H*) as well as systemic injections (Fig. 3*G*). The effects of saline injections were not significantly different between the two genotypes in these tests. Similar results were obtained in both B6/129(F1) and B6/FvB(F1) strains (Fig. S6). Taken together, these results show that the PAG-specific as well as systemic morphine-induced analgesia are substantially impaired in α1G$^{−/−}$ mice.

Low Threshold-Spiking GABAergic Neurons in Both the Wild-Type and α1G$^{−/−}$ PAG Express Functional µORs. PAG cells expected to be responsible for opioid sensitivity are GABAergic neurons (2). We, thus, investigated whether µORs are expressed in these neurons and whether the function of µORs was altered in α1G$^{−/−}$ mice. The FS GABAergic neurons of the ventrolateral (vl)PAG were tested for µOR-induced outward currents, which are known to be mediated by G protein-coupled inwardly rectifying potassium (GIRK) channels (17). We recorded the currents induced by [D-Ala(2),N-Me-Phe(4),Gly(5)-ol]-enkephalin (DAMGO) in the presence of an artificial cerebrospinal fluid (aCSF) inhibitor mixture to inhibit action potentials and synaptic activity. Surprisingly, DAMGO-induced outward currents were only generated in LTS-positive neurons (10.0 ± 2.9 pA, five cells) (Fig. 4*A*); none of the LTS-negative neurons exhibited such currents (0.1 ± 0.1 pA, four cells) (Fig. 4*B*). The frequency of DAMGO-responding (9.5 ± 1.7 pA, six cells) (Fig. 4*C*) or -nonresponding (0.2 ± 0.1 pA; three cells) (Fig. 4*D*) neurons among α1G$^{−/−}$ FS GABAergic neurons was similar to that in the wild type. These
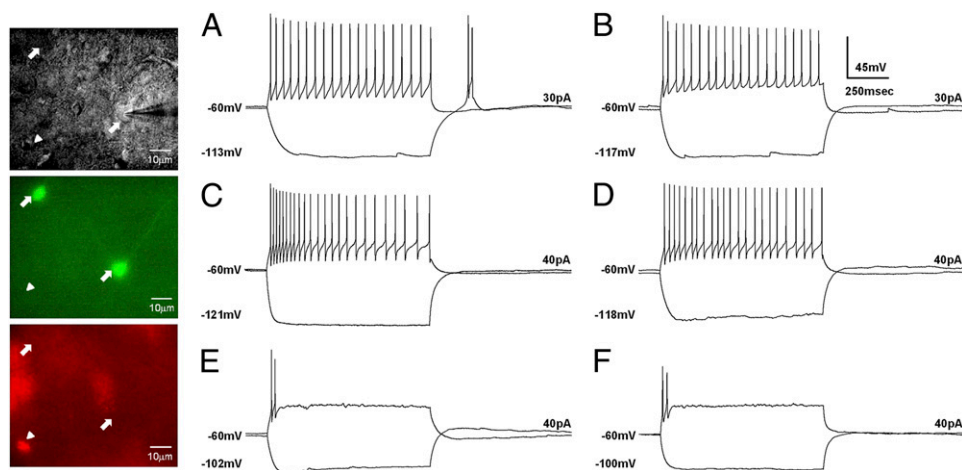
Fig. 2. Electrophysiologically distinct classes of GABAergic neurons and PAG-RVM projection neurons in the vlPAG. The panel displays differential interference contrast (DIC) images (*Top*), GFP images (*Middle*), and retrograde-dye images (*Bottom*) of the patched neurons. Arrows indicate examples of GABAergic neurons, and the arrowhead indicates a PAG-RVM projection neuron. Two response patterns by either negative or positive step-current input are superposed in the traces (*A* and *B*). GABAergic neurons. (*A*) Wild-type LTS-positive FS cells. (*B*) α1G$^{-/-}$ LTS-negative FS cell. (*C–F*) PAG-RVM projection neurons. (*C*) Wild-type FS cells. (*D*) α1G$^{-/-}$ FS cells. (*E*) Wild-type TS cells. (*F*) α1G$^{-/-}$ TS cells. The changes in the membrane potential and the applied currents are indicated in each trace.

data indicate that functional μORs are selectively expressed in low threshold-spiking GABAergic neurons of wild-type mice and are functionally intact in GABAergic neurons of α1G$^{-/-}$ mice, although these latter cells do not exhibit LTS.

Deletion of LTS in μOR-Positive GABAergic Neurons Results in Increased Discharge Activity and Ineffective Inhibition by Endogenous Opioids. T-type channels play crucial roles in the control of cellular-discharge activity (18, 19). Therefore, the deficiency of LTS in the μOR-positive GABAergic neurons of the α1G$^{-/-}$ PAG raised a possibility that the discharge activity of those neurons might have been altered. To test this possibility, we recorded the discharge activity of GABAergic neurons in PAG slices at –50 mV for 1 min. This protocol is based on a previous report that 55% of randomly selected guinea-pig PAG neurons displayed discharge activity at about –50 mV (20). In contrast to guinea-pig PAG neurons, which exhibited discharge activity of ~5 Hz, the discharge activity of GABAergic neurons in wild-type mice was very low, ~0.1 Hz (Fig. 5*C*), likely reflecting species differences. There was no significant difference in the discharge activity between LTS-positive (0.10 ± 0.03 Hz, 13 cells) and -negative (0.08 ± 0.03 Hz, 12 cells) GABAergic neurons in the wild-type mice. In contrast, the α1G$^{-/-}$ GABAergic neurons showed a much wider range of discharge activity, with many neurons showing greater discharge activity than those of wild-type mice (Fig. 5*C*). Hyperexcitable cells, tentatively defined as those exhibiting a discharge activity greater than 0.5 Hz, were only observed in a subpopulation of GABAergic neurons in α1G$^{-/-}$ mice (12/24 cells). These electrophysiological data raised a possibility that LTS was suppressing cellular discharge activity in the LTS-positive subpopulation of GABAergic neurons in the wild-type vlPAG, and deletion of LTS in α1G$^{-/-}$ mice rendered these cells hyperexcitable. This idea was confirmed to be the case as will be described below. However, the discharge activity of projection neurons was not significantly different between wild-type (0.01 ± 0.01 Hz, 12 cells) and α1G$^{-/-}$ (0.04 ± 0.02 Hz, 14 cells) mice.

Next, we examined the sensitivity of wild-type (LTS-positive) and α1G$^{-/-}$ (LTS-negative) GABAergic neurons to the endogenous opioid neurotransmitter [met^5]-enkephalin (ME) based on the results in Fig. 3, because ME is known to be released by stress in vivo and inhibit neurons mostly through μORs (4, 5, 21, 22). After recording basal discharge activity, we applied ME (30 μM) to wild-type low threshold-spiking GABAergic neurons. ME application completely inhibited discharge activity and progressively hyperpolarized the membrane potential

(4.80 ± 0.86 mV) with no apparent recovery of discharge activity, even after washout (Fig. 5*A*). This opioidergic response confirmed that functional μORs are coexpressed with LTS in wild-type GABAergic neurons. In contrast to the wild-type μOR-positive GABAergic neurons, hyperexcitable α1G$^{-/-}$ neurons (i.e., those with basal discharge activity > 0.5 Hz) exhibited greater discharge activity during ME treatment than wild-type μOR-positive GABAergic neurons (Fig. 5*D*) that was followed by a gradual recovery of discharge activity during washout (Fig. 5*B*). Importantly, these hyperexcitable α1G$^{-/-}$ cells were shown to be μOR-positive GABAergic neurons, because ME induced a membrane-potential hyperpolarization (4.59 ± 0.66 mV) like that in wild type and ME significantly suppressed the discharge activity (Fig. 5*D*). However, unlike in the wild type where the discharge activities of GABAergic neurons are fully inhibited by opioid treatments, the partial suppression of the hyperexcitability in the mutant neurons shows that opioid function is limited by the level of discharge activities of those neurons that are controlled by α1G T-type channels.

Increased Frequency of Spontaneous Inhibitory Postsynaptic Currents in α1G$^{-/-}$ PAG-RVM Projection Neurons. The selective hyperexcitability of μOR-positive GABAergic neurons might be expected to translate into greater GABA synaptic transmission to PAG-RVM projection neurons. To test this, we measured spontaneous inhibitory postsynaptic currents (sIPSCs) from PAG-RVM projection neurons in PAG slices (Fig. 6 *A, B, I*). The frequency of sIPSCs in α1G$^{-/-}$ neurons was significantly increased compared with that in wild-type neurons (Fig. 6*C*), whereas the amplitude was not significantly different (Fig. 6*D*). These results indicate that the hyperexcitability of μOR-positive GABAergic neurons caused increased GABA transmission to PAG-RVM projection neurons in the PAG of α1G$^{-/-}$ mice.

To test whether the increased frequency of sIPSCs was attributable to an increase in the number of release sites or release probability (P_r) at the presynaptic terminal, we recorded evoked IPSCs (eIPSCs) (Fig. 6*E*) and the paired-pulse ratio (PPR) of eIPSCs (Fig. 6*G*) in PAG-RVM projection neurons. The maximum amplitudes of eIPSCs and the PPR in the α1G$^{-/-}$ and the wild-type PAG were not significantly different (Fig. 6 *F* and *H*). These findings indicate that the increased frequency of sIPSCs in α1G$^{-/-}$ mice is not because of a change in the number of release sites or P_r and thus, is most likely because of increased discharge activity of GABAergic neurons.
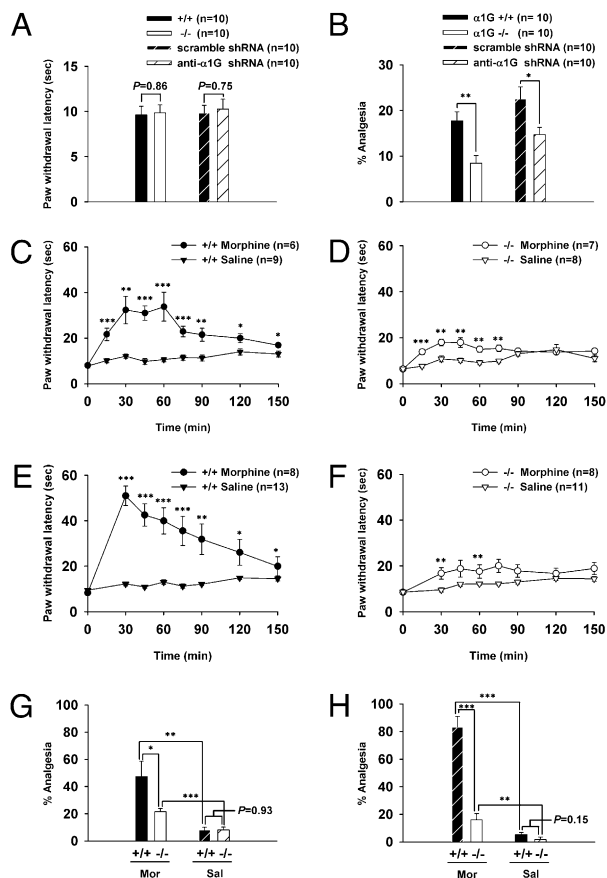
NEUROSCIENCE

Fig. 3. The impaired analgesia in $\alpha 1G^{-/-}$ and PAG-specific $\alpha 1G$-knockdown mice. (*A* and *B*) Bar graphs for the effects of $\alpha 1G$ T-type channels in pain sensation. The wild-type and $\alpha 1G^{-/-}$ mice as well as the scrambled shRNA and shRNA-$\alpha 1G$ mice showed similar basal thermal sensitivity (*A*). The SSIA was impaired in $\alpha 1G^{-/-}$ (17.71% ± 1.98% and 8.44% ± 1.74% analgesia for wild-type and mutant mice, respectively) and $\alpha 1G$-knockdown mice (22.48% ± 2.68% and 14.70% ± 1.66% analgesia for scrambled and shRNA-$\alpha 1G$ mice, respectively) (*B*). (*C*–*F*) Time course for the effects of morphine or saline at the systemic level (*C* and *D*) and the PAG level (*E* and *F*). (*G* and *H*) The percent analgesia at 60 min postinfusion from *C* and *D* are shown in *G*, whereas those at 30 min postinfusion from *E* and *F* are shown in *H*.

The Impaired Analgesia Is Reversed in $\alpha 1G^{-/-}$ Mice by Intra vlPAG Microinjection of Bicuculline. Finally, we examined whether the impaired analgesic effect of locally infused morphine in $\alpha 1G^{-/-}$ mice is a direct result of the hyperactivity of PAG GABAergic neurons. To address this question, we infused morphine (0.6 μg) together with bicuculline (0.6 ng) into the caudal portion of the vlPAG to inhibit GABA$_A$-mediated inhibition and disinhibit PAG output neurons. A lower dose of morphine was used to allow the disinhibitory effect of GABA-receptor antagonism to be observed at the behavioral level. In wild-type mice, as expected, the infusion of the mixture induced greater analgesia than that induced by morphine alone ($F_{1,11} = 6.182$, $P < 0.05$, RM ANOVA) (Fig. 7*A*). However, in mutant mice, not only did the infusion of the mixture induce significantly greater analgesia than that of morphine alone ($F_{1,14} = 7.467$, $P < 0.001$, RM ANOVA) (Fig. 7*B*), it represented a nearly complete restoration of analgesia to wild-type levels ($F_{1,11} = 1.014$, $P = 0.335$, RM ANOVA, shown in Fig. 7 *A* and *B*; $P = 0.72$ at 15 min postinfusion, shown in Fig. 7*C*). Taken together, these results strongly indicate that the increased discharge activity of GABAergic neurons in the vlPAG is solely responsible for the impaired PAG-specific morphine-induced analgesia in $\alpha 1G^{-/-}$ mice.
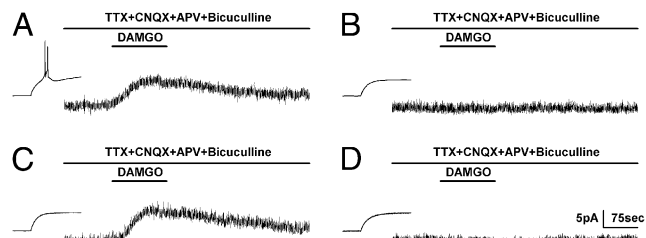

Fig. 4. The selective induction of LTS in μOR-positive FS GABAergic neurons of the vlPAG. The addition of drugs is indicated on top of each trace. (*A* and *B*) Wild-type FS GABAergic neurons. The LTS-positive GABAergic neurons expressed DAMGO-induced outward currents (*A*); none of the LTS-negative neurons showed a response to DAMGO (*B*). (*C* and *D*) $\alpha 1G^{-/-}$ FS GABAergic neurons, both without LTS. The frequency of DAMGO-responding (*C*) and -nonresponding (*D*) neurons among $\alpha 1G^{-/-}$ FS GABAergic neurons was similar to that in the wild-type. Vh, −50 mV.

Discussion

Our current study highlights the $\alpha 1G$ T-type channel of low threshold-spiking GABAergic neurons in the control of opioidergic analgesic signaling in the PAG.

The caudal portion of the vlPAG is the only PAG region in which injections of low doses of morphine produce antinociception (1, 4), but the mechanism responsible for this anatomically restricted effect has remained poorly understood. The FS properties of GABAergic neurons revealed in this study suggest a mechanism for the high opioid sensitivity of this region. The FS properties have been shown to produce proximal inhibitory input with faster kinetics and larger amplitudes, providing both higher temporal fidelity and more powerful inhibitory control over the initiation of action potentials. For example, typical parvalbumin-containing FS neurons constitute only ~1% of the total striatal neuron population (23), but their spikes cause large unitary IPSCs in the striatum that inhibit the majority of the output from this region (24). Therefore, the specific localization
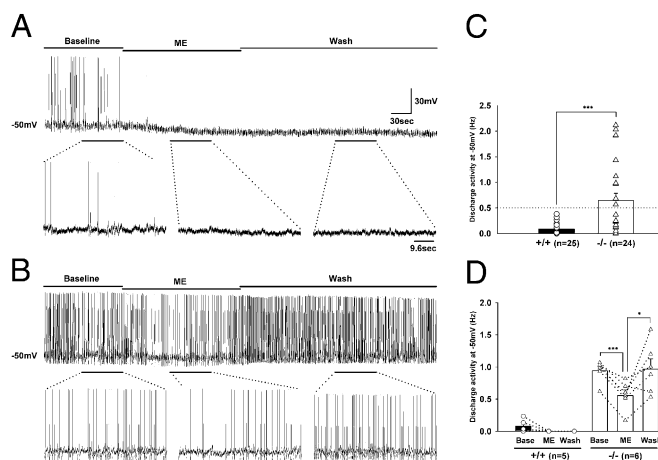

Fig. 5. Discharge activities at a depolarized membrane potential in the μOR-positive GABAergic neurons of the vlPAG. (*A* and *B*) Firing-pattern changes for three periods from (*A*) the wild-type LTS-positive μOR-positive and (*B*) $\alpha 1G^{-/-}$ LTS-negative μOR-positive GABAergic neurons are shown. The portions of the traces underlined by horizontal bars in *A* and *B* were analyzed and presented in *D*. The same portions of the traces are illustrated with an expanded time scale below each trace. (*C*) The bar graph illustrates the basal-discharge activities of wild-type (0.09 ± 0.02 Hz) and $\alpha 1G^{-/-}$ (0.64 ± 0.14 Hz) neurons. (*D*) Changes of discharge activity (*A* and *B*) in the wild-type (basal: 0.08 ± 0.05 Hz; ME: 0 Hz; Wash: 0 Hz) and $\alpha 1G^{-/-}$ (basal: 0.942 ± 0.07 Hz; ME: 0.56 ± 0.09 Hz; Wash: 0.97 ± 0.16 Hz) neurons. Wild type vs. $\alpha 1G^{-/-}$: $F_{1,9} = 66.536$, $P < 0.001$, RM ANOVA. Paired *t* test (*$P < 0.05$; ***$P < 0.001$).
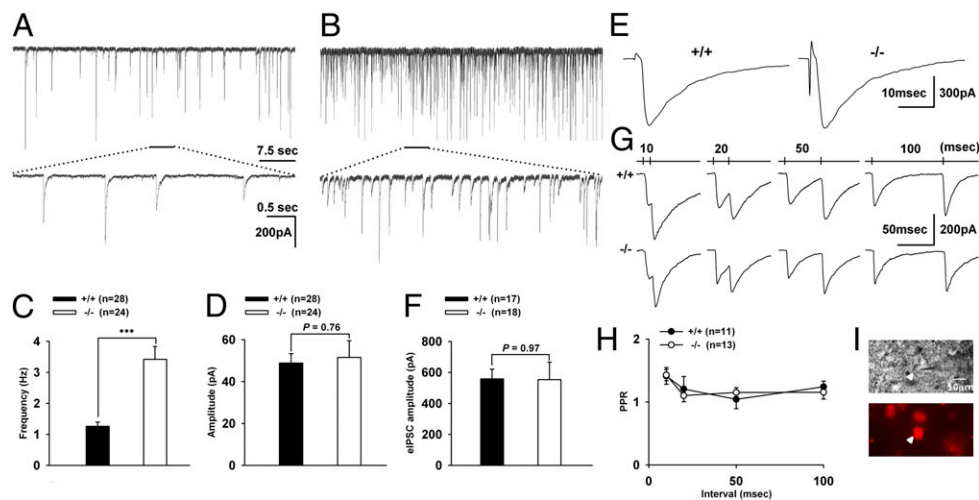
Fig. 6. Characterization of GABAergic sIPSC, eIPSC, and PPR of PAG-RVM projection neurons. (*A* and *B*) Examples of sIPSCs recorded in the wild-type (*A*) and α1G$^{-/-}$ (*B*) projection neurons. Horizontal bars indicate the trace portions that were illustrated with an expanded time scale beneath. (*C*) The bar graph illustrates the frequency of sIPSC in the wild-type (1.26 ± 0.13 Hz) and α1G$^{-/-}$ projection (3.42 ± 0.42 Hz) neurons. The frequency of sIPSC was increased in α1G$^{-/-}$ without changes in the amplitude (48.84 ± 4.45 pA and 51.51 ± 7.98 pA for wild-type and α1G$^{-/-}$, respectively) (*D*). (*E*) Representative traces showing the eIPSC in the wild-type (*Left*) and α1G$^{-/-}$ (*Right*) projection neurons. (*F*) The peak amplitude of eIPSC in the wild-type (558.65 ± 61.94 pA) and α1G$^{-/-}$ projection (553.83 ± 112.34 pA) neurons showed no difference. (*G*) Paired-pulse stimulations elicited eIPSCs that show PPF in wild-type (*Upper*) and α1G$^{-/-}$ projection (*Lower*) neurons. The interstimulus intervals are indicated on the top of the traces. (*H*) The PPR was not significantly different between the two genotypes. (*I*) The DIC image (*Top*) and retrograde dye image (*Bottom*) of a patched neuron. Arrowheads indicate a projection neuron.

of these FS neurons in the caudal portion of the vlPAG may be responsible for the opioid sensitivity of this region.

Our IPSC experiments show that the impaired analgesic response in α1G$^{-/-}$ mice is primarily attributable to enhanced GABAergic inhibition in the PAG. The increased frequency of sIPSCs in α1G$^{-/-}$ mice, together with the absence of any change in sIPSC or eIPSC amplitude or PPR (Fig. 6), indicates that functional T-type channels might be expressed not at the presynaptic axon terminal but probably at or near the soma of low threshold-spiking μOR-positive GABAergic neurons. These findings are consistent with a previous report that α1G T-type channels are prominent in the soma/proximal dendritic region (25).

Basbaum and Fields (5) first proposed a disinhibition model in the PAG in 1984 (Fig. 8*A*), and Jacquet (10) later modified it to explain NMDA-mediated analgesia in 1988 (Fig. 8*B*). The results from our study add a critical dimension to this model by defining a unique population of low threshold-spiking μOR-positive GABAergic neurons expressing α1G T-type channels as the controllers of opioid-dependent analgesia (Fig. 8*C*). α1G T-type channels not only are selectively expressed with μORs in GABAergic neurons of the PAG but also suppress the discharge activities within the range of control by μORs in those neurons to induce opioidergic analgesia. The possible mechanism by which T-type channels are closely linked to μORs may have to do with the fact that opioids hyperpolarize the membrane potential by μORs through GIRK channels (17). This hyperpolarization deinactivates T-type channels, which then can open to cause an LTS. The influxed Ca^{2+} ion through the activated T-type channels might

open other channels, such as Ca^{2+}-activated potassium channels, which are known to mediate slow afterhyperpolarization (AHP) (20, 26, 27). This mechanism may inhibit spike firing in those neurons and decrease GABA release, resulting in disinhibition of the PAG-RVM projection neurons. The other conceivable mechanism is that the long refractory period of LTS (28) might prevent rapidly recurring single firings in those neurons by opioid-induced hyperpolarization. We have previously shown that deletion of T currents in thalamic relay cells results in an increase in single firings (13, 29), whereas enhancing T currents decreases single firings (14). Consistent with this mechanism, we previously observed that thalamic low threshold-spiking neurons of wild-type mice showed longer refractory periods with significantly longer interspike intervals than those of α1G$^{-/-}$ mice (29). Mutant GABAergic neurons might not prevent single firings by opioid-induced hyperpolarization, resulting in enhanced discharge activity (Fig. 8*C*). Collectively, T-type channels and μORs suppress the discharge activity of low-threshold spiking GABAergic neurons in the PAG, resulting in opioidergic analgesia.

PAG regulates pain sensation under stress conditions by inhibiting pain signals at the spinal cord. Previously, we reported that α1G$^{-/-}$ mice showed no impairment in acute pain responses but exhibited hyperalgesia to persistent pain as a reflection of the lack of T-type channel antinociceptive mechanisms in the thalamus (13, 30). The results of the current study suggest a possibility that the hyperalgesia of the α1G$^{-/-}$ mice during persistent pain could be contributed by impaired stress-induced analgesia resulting from the absence of T-type channels in the PAG, implying
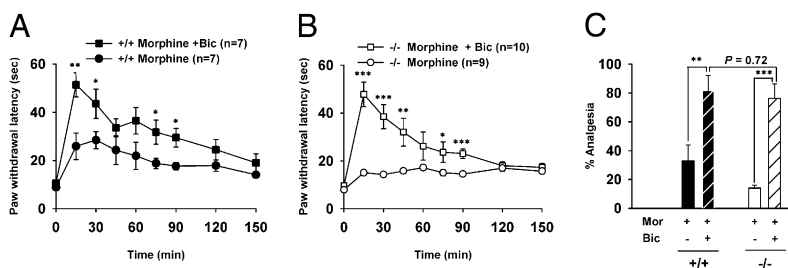

Fig. 7. The reversed opioidergic analgesia by antagonizing local GABA$_A$ receptors in the vlPAG of α1G$^{-/-}$ mice. (*A–C*) The analgesic effects of morphine with or without bicuculline in the vlPAG of wild-type (*A*) and mutant mice (*B*). In mutant mice, the mixture induced a nearly complete restoration of analgesia to the wild-type levels. RM ANOVA and posthoc Tukey test. (*C*) The percent analgesia at 15 min postinfusion from *A* and *B*.
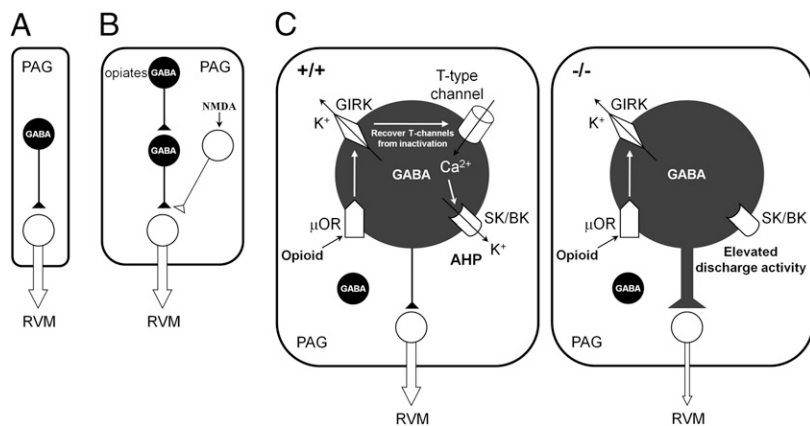
NEUROSCIENCE

Fig. 8. The redefined disinhibition model for the opioid analgesic circuitry in the PAG. (*A* and *B*) The disinhibition model in the PAG was proposed by Basbaum and Fields in 1984 (*A*) and Jacquet in 1988 (*B*). (*C*) The redefined disinhibition model proposed here in wild-type (*Left*) and α1G$^{-/-}$ mice (*Right*); it was reproduced in PAG-specific α1G-knockdown mice. ●, GABAergic neuron; ○, non-GABAergic neuron; ▲, inhibitory; △, excitatory function; ↑, flow of chemicals; ⇓, the excitatory transmission pathways of the PAG-RVM projection neurons. The thickness of the line indicates relative activity of the individual transmission pathway.

that T-type channels in the PAG may suppress persistent pain. Additional studies will be required to better define the antinociceptive function of α1G T-type channels in the thalamus and the PAG during persistent pain. For future studies, we suggest that the current disinhibition model at the PAG provides an improved framework for the development of tools for controlling persistent pain.

Methods

Animals. Male mutants and their wild-type littermates were used for patch-clamp (~4 wk old) and behavioral analyses (12 wk old). Details are provided in *SI Methods*.

Preparation of Brain Slices and Whole-Cell Patch Clamping. Neurons were recorded in acutely isolated PAG slices from ~4-wk-old mice. Details are provided in *SI Methods*.

shRNA and Lentivirus Production. The sequence information on effective shRNA to knockdown α1G was provided by Dr. D. Kim (Korea Advanced Institute of Science and Technology, Daejeon, Korea). Details are provided in *SI Methods*.

Opioid-Dependent Analgesia. SSIA was assessed on the hotplate (52 °C) after a 3-min swim (33 °C). Details are provided in *SI Methods*.

Surgical Preparation for Infusions. All surgeries were stereotaxically performed. Details are provided in *SI Methods*.

In Situ Hybridization and Analysis of α1G Knockdown. We cloned cDNA fragments of mouse *α1G* and the shRNA-mediated α1G-knockdown was analyzed in captured images. Details are provided in *SI Methods*.

Data Analysis. Student *t* test was used unless specified. $P < 0.05$ was considered significant (*$P < 0.05$; **$P < 0.01$; ***$P < 0.001$). All values are expressed as means ± SE. Details are provided in *SI Methods*.

1. Yaksh TL, Yeung JC, Rudy TA (1976) Systematic examination in the rat of brain sites sensitive to the direct application of morphine: Observation of differential effects within the periaqueductal gray. *Brain Res* 114:83–103.
2. Reichling DB, Kwiat GC, Basbaum AI (1988) Anatomy, physiology and pharmacology of the periaqueductal gray contribution to antinociceptive controls. *Prog Brain Res* 77:31–46.
3. Dostrovsky JO, Deakin JFW (1977) Periaqueductal grey lesions reduce morphine analgesia in the rat. *Neurosci Lett* 4:99–103.
4. Lewis VA, Gebhart GF (1977) Evaluation of the periaqueductal central gray (PAG) as a morphine-specific locus of action and examination of morphine-induced and stimulation-produced analgesia at coincident PAG loci. *Brain Res* 124:283–303.
5. Basbaum AI, Fields HL (1984) Endogenous pain control systems: Brainstem spinal pathways and endorphin circuitry. *Annu Rev Neurosci* 7:309–338.
6. Bandler R, Shipley MT (1994) Columnar organization in the midbrain periaqueductal gray: Modules for emotional expression? *Trends Neurosci* 17:379–389.
7. Terman GW, Shavit Y, Lewis JW, Cannon JT, Liebeskind JC (1984) Intrinsic mechanisms of pain inhibition: Activation by stress. *Science* 226:1270–1277.
8. North RA, Williams JT (1983) Opiate activation of potassium conductance inhibits calcium action potentials in rat locus coeruleus neurones. *Br J Pharmacol* 80:225–228.
9. Pan ZZ, Williams JT, Osborne PB (1990) Opioid actions on single nucleus raphe magnus neurons from rat and guinea-pig in vitro. *J Physiol* 427:519–532.
10. Jacquet YF (1988) The NMDA receptor: Central role in pain inhibition in rat periaqueductal gray. *Eur J Pharmacol* 154:271–276.
11. Dogrul A, Zagli U, Tulunay FC (2002) The role of T-type calcium channels in morphine analgesia, development of antinociceptive tolerance and dependence to morphine, and morphine abstinence syndrome. *Life Sci* 71:725–734.
12. Doğrul A, Yeşilyurt O, Işimer A, Güzeldemir ME (2001) L-type and T-type calcium channel blockade potentiate the analgesic effects of morphine and selective mu opioid agonist, but not to selective delta and kappa agonist at the level of the spinal cord in mice. *Pain* 93:61–68.
13. Kim D, et al. (2003) Thalamic control of visceral nociception mediated by T-type Ca2+ channels. *Science* 302:117–119.
14. Cheong E, et al. (2008) Tuning thalamic firing modes via simultaneous modulation of T- and L-type Ca2+ channels controls pain sensory gating in the thalamus. *J Neurosci* 28:13331–13340.
15. Talley EM, et al. (1999) Differential distribution of three members of a gene family encoding low voltage-activated (T-type) calcium channels. *J Neurosci* 19:1895–1911.
16. Kim D, et al. (2001) Lack of the burst firing of thalamocortical relay neurons and resistance to absence seizures in mice lacking alpha(1G) T-type Ca(2+) channels. *Neuron* 31:35–45.
17. Blanchet C, Lüscher C (2002) Desensitization of mu-opioid receptor-evoked potassium currents: Initiation at the receptor, expression at the effector. *Proc Natl Acad Sci USA* 99:4674–4679.
18. Llinás R, Ribary U (2001) Consciousness and the brain. The thalamocortical dialogue in health and disease. *Ann N Y Acad Sci* 929:166–175.
19. Huguenard JR (1996) Low-threshold calcium currents in central nervous system neurons. *Annu Rev Physiol* 58:329–348.
20. Sánchez D, Ribas J (1991) Properties and ionic basis of the action potentials in the periaqueductal grey neurones of the guinea-pig. *J Physiol* 440:167–187.
21. Chieng B, Christie MJ (1994) Hyperpolarization by opioids acting on mu-receptors of a sub-population of rat periaqueductal gray neurones in vitro. *Br J Pharmacol* 113:121–128.
22. Behbehani MM, Jiang M, Chandler SD (1990) The effect of [Met]enkephalin on the periaqueductal gray neurons of the rat: An in vitro study. *Neuroscience* 38:373–380.
23. Rymar VV, Sasseville R, Luk KC, Sadikot AF (2004) Neurogenesis and stereological morphometry of calretinin-immunoreactive GABAergic interneurons of the neostriatum. *J Comp Neurol* 469:325–339.
24. Tepper JM, Bolam JP (2004) Functional diversity and specificity of neostriatal interneurons. *Curr Opin Neurobiol* 14:685–692.
25. McKay BE, et al. (2006) Ca(V)3 T-type calcium channel isoforms differentially distribute to somatic and dendritic compartments in rat central neurons. *Eur J Neurosci* 24:2581–2594.
26. Wolfart J, Roeper J (2002) Selective coupling of T-type calcium channels to SK potassium channels prevents intrinsic bursting in dopaminergic midbrain neurons. *J Neurosci* 22:3404–3413.
27. Smith MR, Nelson AB, Du Lac S (2002) Regulation of firing response gain by calcium-dependent mechanisms in vestibular nucleus neurons. *J Neurophysiol* 87:2031–2042.
28. Jahnsen H, Llinás R (1984) Electrophysiological properties of guinea-pig thalamic neurones: An in vitro study. *J Physiol* 349:205–226.
29. Lee J, Kim D, Shin HS (2004) Lack of delta waves and sleep disturbances during non-rapid eye movement sleep in mice lacking alpha1G-subunit of T-type calcium channels. *Proc Natl Acad Sci USA* 101:18195–18199.
30. Shin HS, Cheong EJ, Choi S, Lee J, Na HS (2008) T-type Ca2+ channels as therapeutic targets in the nervous system. *Curr Opin Pharmacol* 8:33–41.